Fluorescence line-narrowing spectroscopy for probing purposes in bioanalytical and environmental chemistry

Freek Ariese, Arjen N. Bader, Cees Gooijer

Fluorescence line-narrowing spectroscopy (FLNS) is a cryogenic technique that can be used to obtain high-resolution fluorescence spectra. The technique has mainly been used for fingerprint identification. However, this review focuses on the trend to use FLNS for probing purposes: obtaining information on interactions with the local environment or determining conformations.

We briefly discuss the basics of FLNS, solute-matrix interactions and important instrumental aspects. We describe examples from various bioanalytical fields: DNA adducts of the aromatic carcinogen benzo[*a*]pyrene (BP); binding of BP metabolites to monoclonal antibodies or the estrogen receptor; FLNS studies of porphyrin-containing proteins; and, photosynthetic systems.

As an illustration from the field of environmental chemistry, we discuss the use of luminescence line-narrowing spectroscopy – a special mode of FLNS – to study the complexation of lanthanides to humic substances.

Keywords: Benzo[a]pyrene; Cryogenic technique; Estrogen receptor; High-resolution fluorescence; Humic substance; Monoclonal antibody; PAH-DNA adduct; PAH metabolite; Polyaromatic hydrocarbon; Porphyrin

Terms and abbreviations: 3MB, 3-methoxybenzoic acid; Ade, Adenine; ARG, Arginine; BuOH, Butanol; BP, Benzo[*a*]pyrene; CCD, Charge-coupled device; DBalP, Dibenzo[*a,l*]pyrene; DMSO, Dimethylsulfoxide; E2, Estradiol; EEM, Excitation-emission matrix; ER, Estrogen receptor; FLNS, Fluorescence line-narrowing spectroscopy; FWHM, Full width at half maximum; GLU, Glutamic acid; HIS, Histidine; HS, Humic substance(s); IDF, Inhomogeneous distribution function; LLNS, Luminescence line-narrowing spectroscopy; MAb, Monoclonal antibody; MCH, Methylcyclohexane; NMR, Nuclear magnetic resonance; OH-BP, Monohydroxy benzo[a]pyrene; PAH, Polycyclic aromatic hydrocarbon; PSB, Phonon side band; PHE, Phenylalanine; RRS, Resonance Raman spectroscopy; S_0, S_1 etc., Singlet ground state, first excited singlet state, etc.; TEA, Triethylamine; ZPL, Zero-phonon line.

Freek Ariese*, Arjen N. Bader[1], Cees Gooijer
Department of Analytical Chemistry and Applied Spectroscopy, Laser Centre, Vrije Universiteit Amsterdam, De Boelelaan 1083, 1081 HV Amsterdam, The Netherlands

*Corresponding author.
Tel.: +31 20 5987524;
Fax: +31 20 5987543;
E-mail: ariese@few.vu.nl
[1]Current address: Department of Molecular Biophysics, Universiteit Utrecht, Princetonplein 1, 3584 CC Utrecht, The Netherlands.

1. Introduction

Fluorescence spectroscopy is a widely applied analytical tool for selective and sensitive detection of analytes, if needed after fluorophoric or fluorogenic chemical derivatization. It is also a very powerful tool for probing purposes (i.e. for acquiring information about the immediate microenvironment of the fluorescent molecule (see e.g., [1]).

For probing purposes, the fluorescence characteristics – such as quantum yield, wavelengths of excitation/emission bands, fluorescence lifetime or anisotropy – must be sensitive to environmental parameters. Probing may either imply adding a suitable fluorophore to the system of interest, or trying to deduce information about the environment from a molecule of interest that exhibits native fluorescence.

Unfortunately, the wavelength resolution of excitation and emission spectra recorded under conventional conditions (i.e. in the condensed phase at ambient temperatures) is limited. As a result, subtle environment-induced spectral shifts may remain hidden underneath the relatively broad and featureless bands.

It is well known that, under certain conditions, high-resolution, vibrationally resolved fluorescence excitation and emission spectra can be obtained from low-temperature samples. This way, the sensitivity of fluorescence can be combined with the selectivity inherent to vibrational spectroscopies (see e.g., [2]).

0165-9936/$ - see front matter doi:10.1016/j.trac.2008.01.002

Fluorescence line-narrowing spectroscopy (FLNS) is one of these high-resolution fluorescence modes [3–5]. So far, it has mostly been applied for analyte identification purposes, especially in cases where isomer specificity was crucial [4,6,7]. A recent example concerns the determination of fluoroquinolone antibiotics, making use of a combination of line-narrowed spectroscopy at low temperatures and fluorescence lifetimes [8]. For very complex samples, FLNS can be coupled with separation techniques (e.g., thin-layer chromatography [9], liquid chromatography [10] or capillary electrophoresis [11]).

However, in this review, the focus is not on the identification power of FLNS and the spectra as such, but on how these spectra are influenced by the immediate molecular environment of the fluorophoric molecule. In recent years, it was shown that FLNS can be very valuable for probing purposes (e.g., providing detailed information about ligand-biopolymer interactions that could not be readily obtained with other techniques). This will be illustrated for several systems, including DNA adducts of carcinogenic polycyclic aromatic hydrocarbons (PAHs) and their metabolites. We will explain how FLNS can be used to study binding modes to DNA, or to elucidate the predominant interactions with monoclonal antibodies (MAbs) or with protein receptors. Even enantiospecific spectral differentiation of stereoisomeric metabolites has been achieved. Other examples include porphyrin studies, photosynthetic systems, and the assessment of crystal field strengths in lanthanide-humic acid complexes.

It is the aim of this review to explain how environment-induced shifts can be studied at cryogenic temperatures, and how FLNS spectra can provide information on probe interactions with its immediate environment.

FLNS has also been used extensively in physical chemistry studies (e.g., impurities in crystals [12], laser materials [13], and polymer gels [14]). However, the focus of this review is on life sciences and environmental applications.

2. FLNS basics

2.1. Conventional fluorescence, broadening effects and probing

Consider an organic, fluorophoric molecule in liquid (or solid amorphous) solution. The electronic transitions responsible for the absorption and fluorescence spectra of such a compound are usually illustrated by a simplified Jablonski energy diagram, in which the electronic states (and the associated vibrational states) are indicated by separate horizontal lines. Absorption transitions typically start at the lowest vibrational level of the electronic ground state, S_0. After fast non-radiative decay (including vibrational relaxation and energy interconversion), fluorescence transitions start from the lowest vibrational level of the first excited singlet state, S_1 (Kasha's rule). In view of this scheme, one might expect to observe sharp lines, with the excitation spectrum showing the vibrations of the molecule in the electronically excited states, and the emission spectrum showing the vibrations of the molecule in the ground state. However, normally only a broad envelope is observed, showing little or no vibrational structure.

One of the causes of spectral broadening is that the Jablonski scheme applies to an individual molecule, whereas, in practice, we usually observe the emission from a large ensemble of fluorophores, with each individual molecule experiencing its own particular interactions with the surrounding solvent or matrix. In other words, in liquid solutions or in solid, amorphous samples, the vibronic transitions of a fluorophore are inhomogeneously broadened, due to the variability in the local environment (either continuously changing or immobilized). Furthermore, at ambient temperatures, each individual molecule will show homogeneously broadened transitions as a result of electron-phonon coupling with the surrounding matrix (see further below). Circumventing such broadening effects is a crucial aspect of the research described in this review.

A change in environment can induce spectral shifts if the probe-matrix interactions are not identical for the corresponding electronic states. In fact, the electronic distributions are often very different. Suppose, for instance, that the molecule has a larger electrical dipole moment in the S_1 state than in the S_0 state. In a polar solvent, this S_1 state will be more stabilized than the ground state. As a result, upon increasing the solvent polarity, a red shift in fluorescence emission should be expected, provided that the required reorganization of the surrounding solvent molecules can be achieved within the lifetime of the excited state. Thus, spectral changes provide information on the nature of the solvent environment (e.g., polarity probes). Of course, this effect will be very different in frozen solutions, where solvent reorganization is inhibited.

The extent of the shift is, of course, dependent on the fluorophore. In cases where the excited state has a charge-transfer character, they can be dramatic: Stokes' shifts up to 10,000 cm^{-1} (150–200 nm) have been reported [15]. However, most fluorescent compounds show only minor solvent shifts of the order of a few nm, and they are of limited use as environment-sensitive probes under conventional, low-resolution conditions. However, it will be shown that, in FLNS, under low-temperature conditions, minor shifts are much more readily detected and can provide a wealth of information.

2.2. High-resolution fluorescence

In order to obtain high-resolution molecular fluorescence spectra in the condensed phase, the effect of

inhomogeneous broadening must be reduced as much as possible. Apart from single-molecule spectroscopy [16], there are basically two approaches [5,17,18]:

- Shpol'skii spectroscopy; and,
- FLNS.

In Shpol'skii spectroscopy, a polycrystalline matrix is used (typically a frozen *n*-alkane), in which the individual fluorophores occupy specific, well-defined sites and experience (practically) the same analyte-solvent interaction. This approach works best for rigid, non-polar compounds and has proved useful for ultra-sensitive analytical measurements of carcinogenic PAHs [19] or photophysical studies [20].

However, for probing purposes, one would prefer a method that is more broadly applicable. That is why, in the present paper, we focus on FLNS, since this high-resolution technique can be applied to many types of amorphous or glassy matrices at cryogenic temperatures, and also in cases where the fluorophore can adopt a broad distribution of orientations (e.g., biopolymers in aqueous environments [5,21]). The fluorophore ensemble will experience a broad range of different solvent environments (similar to the situation at room temperature), but, in a cryogenic matrix, this environment is not likely to change during the lifetime of the excited state.

The first FLNS spectra were recorded in the 1970s by Personov and co-workers [22,23], and its working principle is illustrated in Fig. 1. Excitation is usually carried out with a laser at a wavelength coinciding with an S_0–S_1 vibronic transition. From the inhomogeneous population of molecules, only a minor fraction of fluorophores is excited, possessing vibronic transition energies matching the photon energy of the laser. This sub-selection or ''isochromat'' will still experience similar matrix-interaction energies after vibrational relaxation. In other words, the higher vibrational levels and the v = 0 level of the S_1 state are correlated. Since only the molecules of this isochromat will emit fluorescence, this will result in a line-narrowed emission spectrum [3,5].

The relative intensities of the narrow lines not only depend on the absorption cross-section of the vibronic transition but also on the position of the laser wavelength in the inhomogeneously broadened absorption band. In a crowded part of the absorption spectrum, the spacing between vibronic bands will be smaller than the inhomogeneous broadening, and more than one vibronic transition will be excited simultaneously. This is illustrated in Fig. 1, where three bands overlap with the laser line, each belonging to a different isochromat. As a result, we will obtain three narrow 0,0 lines in emission. The energy difference between the excitation wavelength and each of the narrow lines in the origin multiplet corresponds to the excited state vibrational energies of the analyte. This feature of FLNS has proved extremely

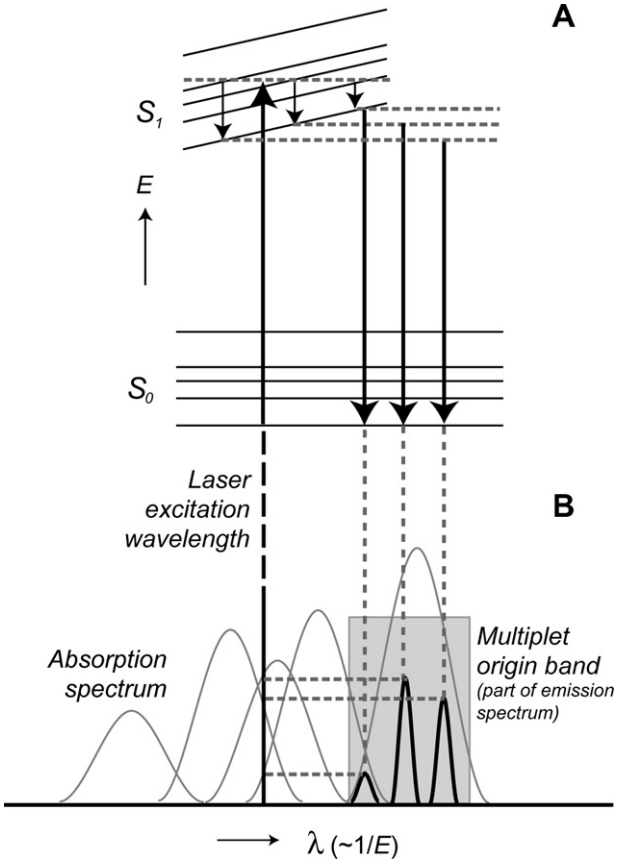

Figure 1. Jablonski diagram illustrating the range of S_0–S_1 energy differences, the three isochromats selected by the laser in FLNS (A), and the resulting spectrum (B). The slanted levels of the S_1 state indicate the inhomogeneous broadening.

useful for the fingerprint identification of closely related compounds [3,4,6,10,24]. The role of FLNS in the elucidation of DNA-adduct formation by PAHs and by endogenous estrogens was reviewed recently [7].

A background-free multiplet origin band, as shown in Fig. 2, is rarely observed in practice; often a broad, red-shifted background is also observed. This is due to electron–phonon coupling (i.e. coupling of electronic transitions of the fluorophore with lattice vibrations of the matrix (phonons) [5]). This interaction results in a broad phonon side band (PSB), red shifted from the narrow zero phonon line (ZPL). The intensity of the PSB compared to that of the ZPL increases with temperature and with the strength of the solvent–solute interaction. In order to obtain highly resolved spectra, the measurement temperature should therefore be as low as possible (typically 10 K or lower), although for some solute–solvent combinations, where the coupling is too strong, even at such extremely low temperatures, no FLN spectrum can be obtained. The intensity of the sharp ZPL relative to the broad PSB is of great diagnostic value: it can serve as an indication of the type and the strength

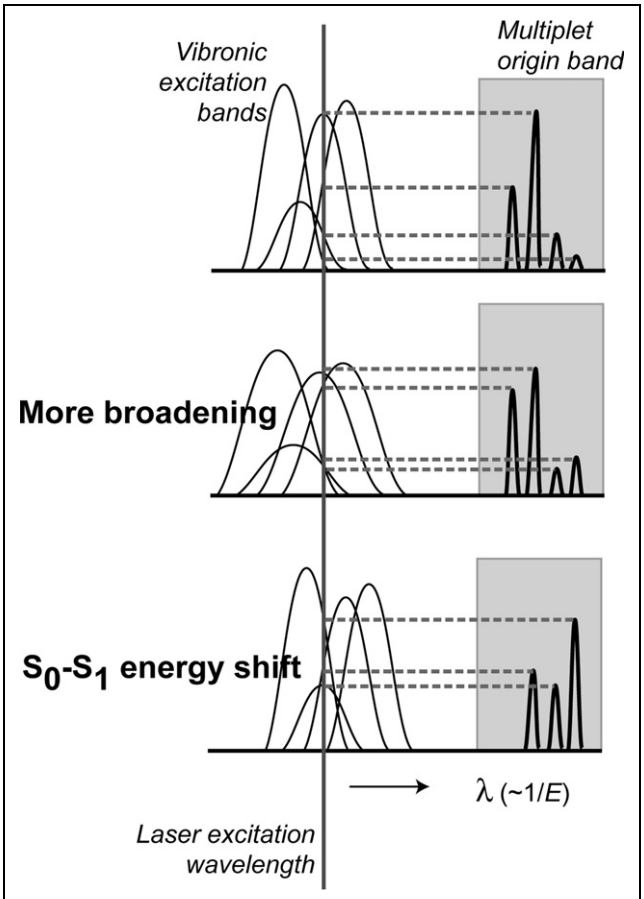

Figure 2. Solvent dependencies in FLNS spectra. Overlap of the laser with four vibronic bands is shown, resulting in four narrow bands in the multiplet origin band (top). More broadening of the vibronic bands in excitation (middle) or a red shift in S_1-S_0 energy (bottom) results in a change in the relative intensities of the ZPLs in emission (adapted from [25], with permission).

of the interaction of the solute with its immediate environment [5,21].

2.3. Solvent effects on FLNS

As regards solvent-induced spectral shifts at low temperatures, it should be recalled that solvent reorientation is largely prohibited in frozen matrices. Thus, under such conditions, solvent-induced blue or red shifts in excitation and emission are the result of interactions corresponding to the ground-state conformations (similar to absorption transitions). The absence of reorientation effects means that these shifts are often more straightforward to interpret than in liquid-phase experiments. Furthermore, owing to the high spectral resolution, even minor shifts will show up very clearly in the multiplet origin band. This is schematically illustrated in Fig. 2, where four (S_1 state) vibrations are considered [25]). The top frame corresponds with a ''normal'' reference solvent. When the solute–solvent interaction (or more precisely the variation in solute–solvent interactions (e.g., in polar media)) results in more inhomogeneous broadening, the ZPLs at both edges of the multiplet will increase in intensity (middle frame). A red shift results in an increase of the relative intensities of the ZPLs at the red edge of the multiplet and a decrease at the blue edge (bottom frame). The opposite will be observed for a blue shift (not shown). Furthermore, the strength of electron-phonon coupling (ZPL/PSB ratio) depends on the strength of the interaction between solute and solvent.

2.4. General instrumental requirements

For FLNS measurements, a laser system is needed that can be tuned over the vibronic region of the S_0–S_1 absorption band of the compound of interest. Excitation into higher electronic states does not result in line narrowing: electronic states are not correlated, so individual molecules that happen to possess identical S_0–S_2 transitions will normally lose their isochromatic properties upon relaxation to S_1. Furthermore, lifetime broadening at higher electronic states will limit the spectral resolution. For the same reason, ultrashort laser pulses should be avoided; most researchers use excimer-pumped dye lasers with ns pulses.

For cooling the samples, either helium bath cryostats or closed-cycle refrigerators can be used. Nowadays, the latter can also reach temperatures of 4–5 K and tend to be less expensive since no liquid helium is consumed. However, bath cryostats allow one to change samples within minutes, whereas, in a closed-cycle system, a cool-down time of an hour or longer may be required to cool one or a few samples. An interesting new approach was developed by Bystol and Campiglia [26], who constructed a fiber-optic probe that can simply be plunged into a helium-storage Dewar.

For detection, a spectrograph with a CCD detector is required with a spectral resolution of 0.05 nm or better. In the case of pulsed laser excitation, an intensified CCD can be operated in the gated mode in order to reject Rayleigh scatter and reflected laser light. For technical details, the reader is referred to the original publications.

3. FLNS for probing purposes

3.1. PAH-DNA adduct conformations

The use of FLNS for probing purposes has attracted attention in the recent literature. At Iowa State University, the group of Ryszard Jankowiak and the late Gerald J. Small extensively studied the spectra of PAHs, in particular the strong environmental carcinogens benzo[*a*]pyrene (BP) and dibenzo[*a,l*]pyrene (DBalP), as well as their adducts to DNA.

Using BP-DNA adducts bound to a specific guanosine in synthetic oligomers, Suh et al. studied the conforma-

tion (intercalated vs. base-stacked vs. solvent-exposed) as a function of base sequence [27] and as a function of adduct stereochemistry [28]. Intercalation of the adduct (and thus strong π–π interactions with neighboring DNA bases) was indicated by strong PSBs in the FLN spectra. The spectroscopic results obtained in frozen aqueous buffer agreed well with room-temperature fluorescence-quenching studies and with 3D NMR results, indicating that the conformations observed in frozen matrices are comparable to those observed under ambient conditions.

In a separate study, it was found that conformations play an essential role in cancer initiation. In mouse skin following topical application of BP, external, solvent-exposed BP-DNA adducts were more quickly repaired than base-stacked adducts [29]. More recently, stereoisomeric and conformational analysis of BP-DNA adducts by FLNS in lung tissue of mice was reported by Banasiewicz et al. [30].

3.2. PAH binding to antibodies

Next, we discuss the use of FLNS as a tool to study binding to MAbs, which are frequently used as a preconcentration step (e.g., for the selective isolation of PAH metabolites and PAH-DNA adducts from urine [31]). The metabolite (+)-*trans-anti*-7,8,9,10-benzo[*a*]pyrene-tetrol (BP-tetrol), is formed upon monooxygenation and hydrolysis. The adduct 7-(benzo[*a*]pyren-6-yl)guanine (BP-6-N7Gua) is formed upon one-electron oxidation of BP, reaction with the DNA-base guanosine and subsequent depurination. Both compounds (see Scheme 1 for structures) can be used as urinary biomarkers; BP-tetrol is a biomarker of exposure and metabolism, whereas BP-6-N7Gua is a biomarker of actual DNA damage [7,32].

In order to characterize the binding mode to their respective MAbs, FLN spectra of MAb-bound BP-tetrol and BP-6-N7Gua were compared to their spectra in various solvent environments. For BP-tetrol, the stereochemistry of its four hydroxyl groups attached to the saturated ring (*cis* vs. *trans* configurations) has a major effect on the FLNS spectrum [33] and an influence of H-bonding solvents can be expected. In the case of BP-6-N7Gua, the only H-bonding atoms are located on the guanine moiety and any effect on the fluorophore from H-bonding is expected to be very minor. However, earlier studies on intercalated BP-DNA adducts showed that π-π interactions can have a strong effect on the FLNS spectra, presumably due to the S_1 state of the fluorophore having a charge-transfer character [28].

In Fig. 3, major differences in the relative intensities of the BP-tetrol bands are observed for different solvents [34]. The FLNS spectra show the 0,0 region with pronounced ZPLs, after subtraction of a relatively weak,

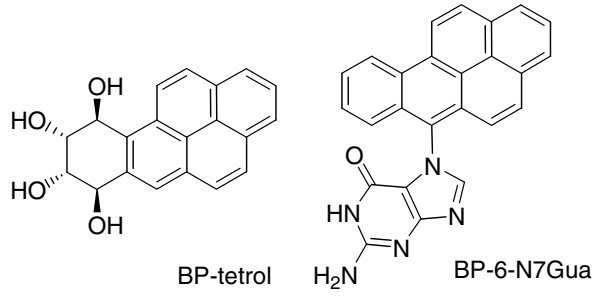

Scheme 1. Structures of (+) *trans-anti*-BP-tetrol and BP-6-N7Gua. In the case of BP tetrols, *trans* refers to the relative configuration of 9-OH and 10-OH, whereas *anti* refers to the relative configuration of 7-OH and 9-OH. In total, four pairs of *anti* stereoisomers exist (7-OH and 8-OH are always *trans*).

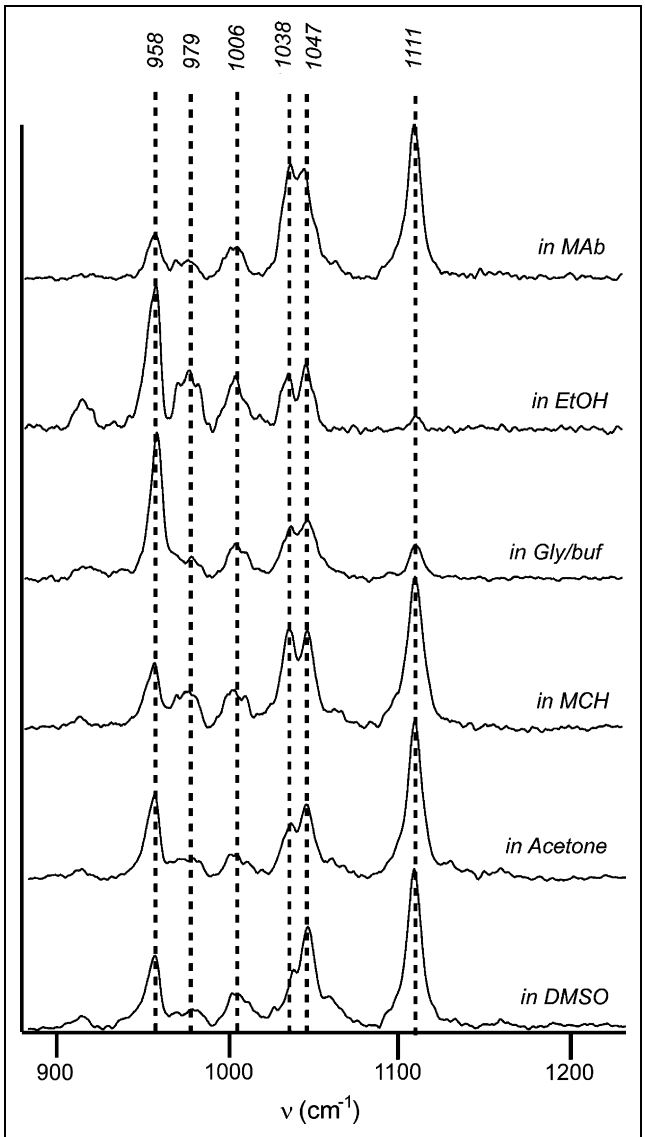

Figure 3. FLNS spectra of BP-tetrol inside the MAb and in various solvents (ethanol, glycerol/buffer, methylcyclohexane, acetone, dimethylsulfoxide). The spectra show the background-subtracted origin region, excited at 363.0 nm. The numbers labeling the ZPLs are the S_1 state vibrational energies in cm^{-1} (from [34], with permission).

broad fluorescence background. This background is due to phonon sidebands (*vide supra*) and can also provide valuable information on solute–matrix interactions [34]. The positions of the ZPLs are virtually identical in the different solvents (experimental uncertainty ±3 cm^{-1}), indicating that the intramolecular vibrational energies of the S_1 state are not significantly affected by the environment. When comparing the relative intensities of the ZPLs, it can be seen that the FLNS spectrum of BP-tetrol is hardly influenced by the dielectric constant (ϵ_r) of the solvent: in aprotic polar solvents (e.g., acetone ($\epsilon_r = 20$) and DMSO ($\epsilon_r = 47$)) and in non-polar solvent methylcyclohexane (MCH, $\epsilon_r = 2$), similar spectra were obtained.

However, the ZPL-intensity distributions for the aprotic solvents differ significantly from those observed with H-bonding solvents ethanol and 50/50 glycerol/buffer. This is most evident by comparing the intensities of the ZPLs at 958 and 1111 cm^{-1}. For BP-tetrol in H-bonding solvents, the excited state mode at 958 cm^{-1} is much more intense than the mode at 1111 cm^{-1}.

In the aprotic solvents MCH, acetone and DMSO, the opposite is observed. Thus, H-bonding leads to a blue shift of the S_0–S_1 transition, in full agreement with Hayes et al. [35].

Summarizing, from the similarity of the spectra in MCH with those of the MAb complex, it can be concluded that the binding mechanism inside this MAb is of a non-polar character, and that H-bonding and π–π interactions do not play a major role in antigen binding. Using a similar approach, it was found that the binding mode of the MAb raised against the depurinating adduct BP-6-N7Gua involves π-π interactions (spectra not shown) [34].

With the help of MAbs, Grubor and co-workers were even able to differentiate between the four isomers of *anti*-BP-tetrol (i.e. (±)-*cis*- and (±)-*trans*-*anti*-BP-tetrol [36]). For the *cis* and *trans* forms, the S_1 vibrations are quite different and they are easily distinguished in FLNS [33], but, as expected, the spectra of the optical isomers are identical for the unbound ligands (See Fig. 4, top spectra). However, upon complexation to the antibody, FLNS spectra with clearly different band intensities are also obtained for the optical isomers (Fig. 4, lower spectra), as a result of different ligand–protein interactions. In other words, binding to the non-symmetrical MAb results in the formation of diastereoisomeric complexes. These results are in agreement with those of Suh et al. [28], who observed similar effects upon binding to DNA oligomers.

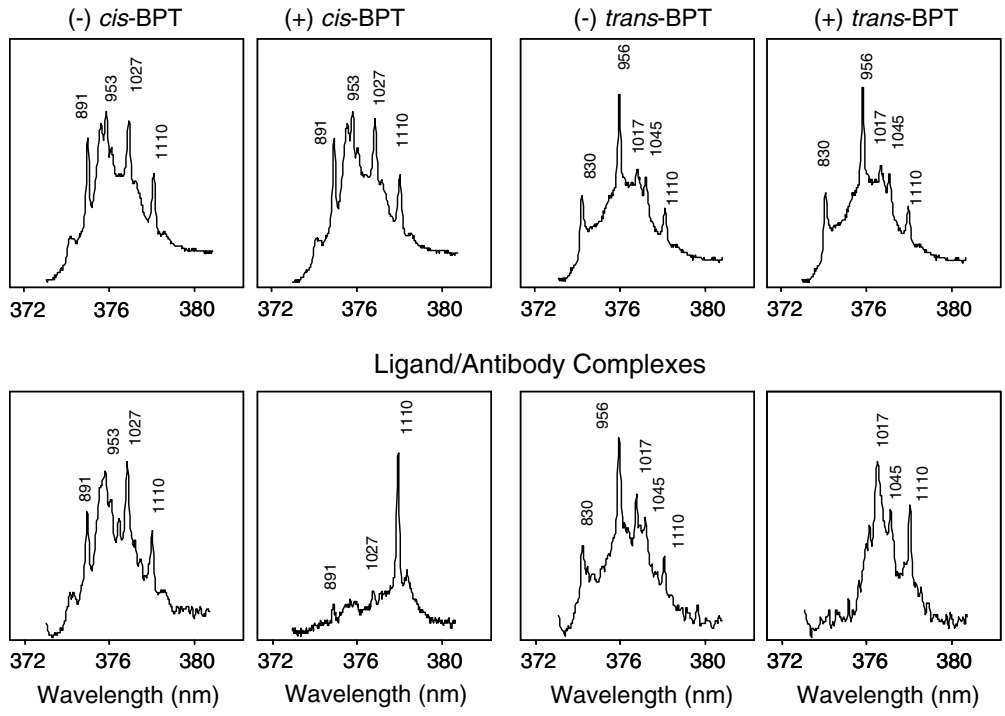

Figure 4. FLNS spectra of four stereoisomeric BP-*anti*-tetrols, as unbound ligands (top frames) and bound to MAb (bottom frames). Upon binding to MAb, all four isomers can be distinguished as a result of specific interactions. Peak labels correspond with S_1 vibrational energies in cm^{-1} (adapted from [36], with permission).

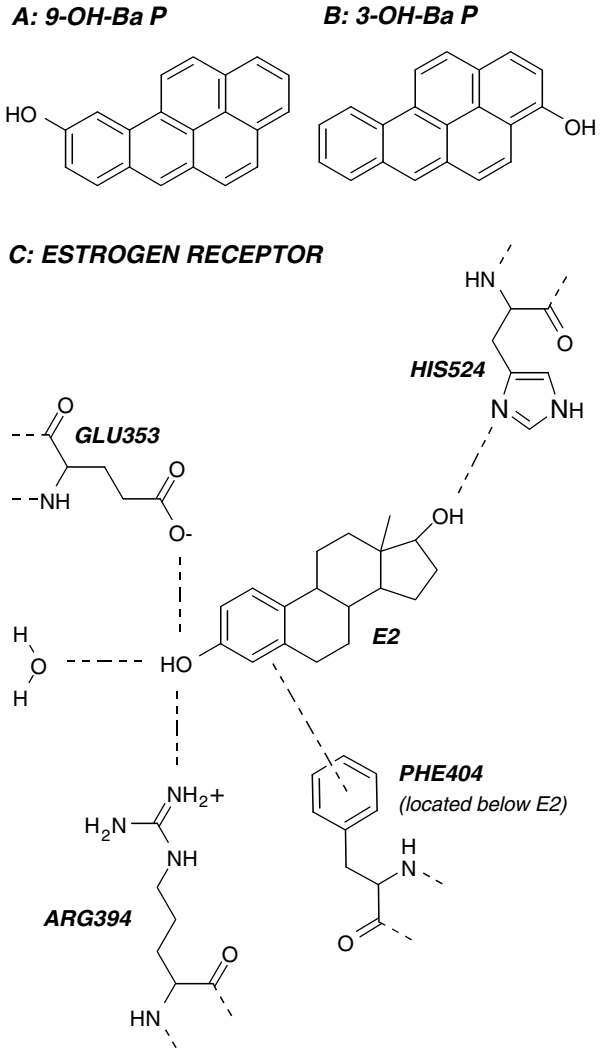

Figure 5. The molecular structure of 9-OH-BaP (A), 3-OH-BaP (B), and estradiol (E2) located in the estrogen receptor (ER) binding pocket (C). The amino acids shown are involved in the binding of E2 to the ER (from [25], with permission).

Important for identification is the fact that vibrational frequencies are usually not affected. FLNS was also able to shed light on cross-reactivity and multispecific functionality of MAbs [37], a feature that plays a central role in immuno-analytical techniques and, of course, also in the functioning of the immune system.

3.3. PAH binding to the estrogen receptor

In a recent paper, FLNS was applied to study the chemical interactions between xeno-estrogenic ligands and the estrogen receptor (ER) [25]. Earlier, BP had been found to exhibit estrogenic activity in various *in vitro* and *in vivo* systems following metabolism [38,39]. For several mono-hydroxylated BPs (i.e. 2-OH-, 3-OH-, 8OH- and 9-OH-BP), low-affinity but nevertheless relevant estrogenic activity was reported. The structural resemblance of 3-OH-BP and 9-OH-BP with the endogenous estrogen 17β-estradiol (E2) is evident from Fig. 5. For E2, the binding orientation in the ER is known from crystallographic data [40]. However, it is difficult to predict binding modes (and affinities) of ligands (e.g., the OH-BPs), since they possess only one hydroxy-group, which may be directed either towards GLU353 and ARG394, or towards HIS524.

Analogous to the procedure described above, FLNS spectra of 3-OH-BP and 9-OH-BP (selected because of their higher natural abundance) were recorded in various solvent mixtures, and compared with the spectrum obtained for the ER-bound ligand. The solvents selected were representative for hydrophobic interaction (MCH), H-bond accepting interaction (triethylamine/TEA), both H-bond accepting and donating interaction (butanol/BuOH), aromatic π-electron interaction (toluene) and carbonyl π-electron interaction (acetone). After baseline correction, both for 9-OH-BP and 3-OH-BP, highly resolved spectra could be obtained (not shown).

A detailed analysis of the solvent influences was conducted by comparing the relative contributions of characteristic vibrational peaks, as shown in Table 1 for 9-OH-BP. It was concluded that 9-OH-BP interacts with an H-bond acceptor (i.e. the imidazole moiety of HIS524). Furthermore, the spectra indicate that 9-OH-BP interacts with a toluene-like moiety in the ER (i.e. PHE404) in a π–π stacking manner.

From a similar inspection of the 3-OH-BP spectra, Bader and co-workers [25] concluded that the spectrum in the ER complex is most similar to the one in the presence of TEA, indicating interaction with an H-bond acceptor (i.e. the imidazole moiety of HIS524).

Such experimental results are an important addition to the modeling data reported in the literature. For endogenous estrogen E2, the contributions of the two H-bonds to the total receptor/ligand binding energy have been estimated, showing that the participation of E2's phenolic OH-group in the H-bonding network with GLU353 and ARG394 contributes to a larger extent than the H-bond donated to the HIS524 [41]. For both mono-hydroxylated BPs studied here, our results strongly suggest that H-bonding with HIS524 is the predominant interaction, in line with the molecular modeling data of Van Lipzig et al. [42]. The latter study also predicted interaction with PHE404, which is confirmed by the FLNS data.

3.4. Porphyrins and photosynthesis studies

FLNS can also be a valuable technique when studying the relationship between protein structure and protein function. By recording the changes in the spectrum of a chromophore as a function of changes in the protein matrix, one can obtain information on the interactions that have a direct impact on that chromophore, which

Table 1. Spectral shifts in the FLN spectrum of 9-OH-BaP in the presence of the estrogen receptor (ER) and in a number of solvent combinations. Relative intensities of five peaks in the multiplet origin region: (A) 840 cm^{-1}; (B) 980 cm^{-1}; (C) 1050 cm^{-1}; (D) 1177 cm^{-1}; and, (E) 1328 cm^{-1}(from [25])

	Solvent	A	B	C	D	E
Estrogen Receptor						
-ER present	*ER in Glycerol/Buffer*	2	2	7	6	10
-ER absent	*Glycerol/Buffer*	10	3	3	0	0
Hydrophobic interaction						
- reference	*MCH*	1	2	10	6	2
H-bonding interaction	*MCH*					
-with GLU & ARG	*+Butanol*	3	2	10	5	2
-with HIS	*+TEA*	2	1	10	10	8
π–π interaction	*MCH*					
-with PHE	*+Toluene*	1	2	10	7	6
-with C=O	*+Acetone*	4	6	10	6	4
Both H-bonding and π–π interaction	*MCH*					
-with PHE and GLU & ARG	*+Toluene + Butanol*	2	2	10	6	2
-with C=O and GLU & ARG	*+Acetone + Butanol*	2	3	10	6	3
-with PHE and HIS	*+Toluene +TEA*	2	2	9	9	10
-with C=O and HIS	*+Acetone +TEA*	5	2	7	8	10

MCH, Methylcyclohexane; TEA, Triethylamine.

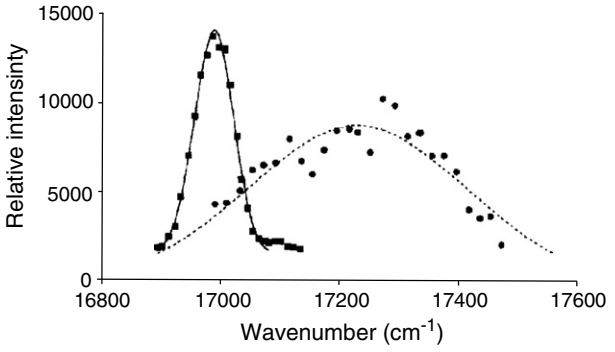

Figure 6. Distribution function of the 0,0 transitions of Zn cytochrome *c* in its native state (squares, fitted with full line) and after denaturation (circles, fitted with dashed line); T = 4.2 K (from [45], with permission).

one cannot always be deduced from the three-dimensional structure of the protein (if known at all).

Vanderkooi and co-workers have reported extensively on the use of FLNS for porphyrin studies [21,43,44]. In most of these studies, fluorescence quenching was avoided by replacing the central Fe ion by Zn(II) or Mg(II). By monitoring the intensity of a specific ZPL as a function of excitation wavelength, one can determine the inhomogeneous distribution function (IDF) of the 0,0 transition, free of phonon-broadening, temperature effects and solvent reorientation. The experiment can be understood on the basis of Fig. 2: by slowly scanning the laser excitation wavelength through an inhomogeneously broadened vibronic band, the corresponding ZPL in emission will trace this band shape. During the scan, care should be taken to correct for possible variations in laser intensity. From the width of the IDF, one can deduce the level of heterogeneity of the protein environment surrounding the chromophore: a narrower IDF means a high level of structure. A protein environment has glass-like, amorphous properties, but there is a higher level of structure than in a random solvent matrix [21]. As an example, Fig. 6 shows that the width of the IDF of Zn(II) cytochrome *c* is 65 cm^{-1} in its native state (full line). When a denaturant was added to the sample before freezing to 4 K, a much broader band (dashed curve; width 361 cm^{-1}) was observed, indicating a strongly inhomogeneous environment [45].

When the IDF cannot be fitted with a single Gaussian curve, it is an indication that more than one distinct species is present (e.g., in the case of endogenous porphyrins in *E. coli* bacteria, the IDF showed the existence of at least 5 distinct species [46]).

Laberge and co-workers [47] used FLNS to study the binding of benzohydroxamic acid and naphthohydroxamic acid to horseradish peroxidase *c*. In this case, the authors focused on changes in vibrational frequencies rather than changes in IDF or ZPL/PSB ratios and concluded that the central Mg(II) ion was 5-coordinated in all cases (i.e. no water ligand).

In the field of photosynthesis, Gall and co-workers [48] applied FLNS and resonance Raman spectroscopy (RRS) to light-harvesting protein LH2 of the bacterium *Rhodopseudomonas acidophila*. Bacteriochlorophyll *a* had been replaced with chlorophyll *a* (Chla) to study the energy transfer mechanism, and the FLNS spectra were used to

demonstrate the correct incorporation of the Chla molecules. For these systems, FLNS resulted in spectra with a far superior signal-to-noise ratio than RRS. In an FLNS study by Peterman and co-workers on the isolated reaction center of photosystem II, it was found that emitting and charge-separating states are very similar, as concluded from the similarities in vibrational frequencies, phonon sidebands, and the double-Gaussian shape of the IDFs [49].

3.5. Luminescence line narrowing spectroscopy

Complexation is also of major importance in environmental chemistry. Kumke and co-workers used FLNS to shed light on the binding of chemicals to humic substances (HS), a key step for pollutant transportation in rivers, lakes and aquifers. In an earlier study, pyrene was selected as a model compound for organic, non-polar pollutants [50]. More recently a completely different approach was used, namely (luminescent) Eu complexes with the objective to study the binding of heavy-metal ions with HS [51]. Due to the presence of a large number of ionic or highly dipolar functional groups (mainly carboxylic and phenolic groups), HS are able to form strong complexes with metal ions, and thus determine the species distribution of the metal ions in the environment [52]. Eu(III) is a natural analogue of actinides (An(III)), which makes it very attractive as a surrogate in the investigation of actinide migration in the environment (e.g., through geological barriers of nuclear waste repository sites). Furthermore, because of its outstanding luminescence properties, it can be used to probe the molecular environment in metal–HS complexes [53,54]. The observed spectral features as well as the luminescence decay time of Eu(III) are directly correlated with the complex formed. Depending on the experimental set-up, information about the stoichiometry, geometry and stability of the complex can be obtained [53]. In a strict sense, the emission monitored here is not fluorescence, and the more appropriate term is luminescence line-narrowing spectroscopy (LLNS). Focus was on the largely forbidden radiative atomic transitions from the $^5D_0$-level to the $^7F_1$ and $^7F_2$ levels of Eu^{3+}. Direct $^5D_0 \leftarrow {}^7F_0$ excitation was applied (see Fig. 7), even though the extinction coefficient is extremely small due to parity forbiddance. Since this transition is non-degenerate, and thus not split by the crystal field (Stark splitting), its energy is characteristic for a specific complex. The appearance of more than one band in excitation directly indicates the presence of more than one species. At room temperature, such effects often go unnoticed because of band broadening.

LLNS offers unique possibilities for the characterization of Eu(III) complexes with HS and with simple model ligands. In Fig. 8, part of the excitation-emission matrix (EEM) of a Eu(III) complex with 3-methoxybenzoic acid (3MB) recorded is shown. The $^5D_0 \rightarrow {}^7F_1$ transition is observed in emission (588–596 nm), while scanning the excitation wavelength over a relatively narrow range (579.20–579.55 nm). The $^5D_0 \leftarrow {}^7F_0$ excitation band appears as an asymmetric broad band of ca. 0.2 nm FWHM, indicating the presence of more than one species (see Fig. 8, top).

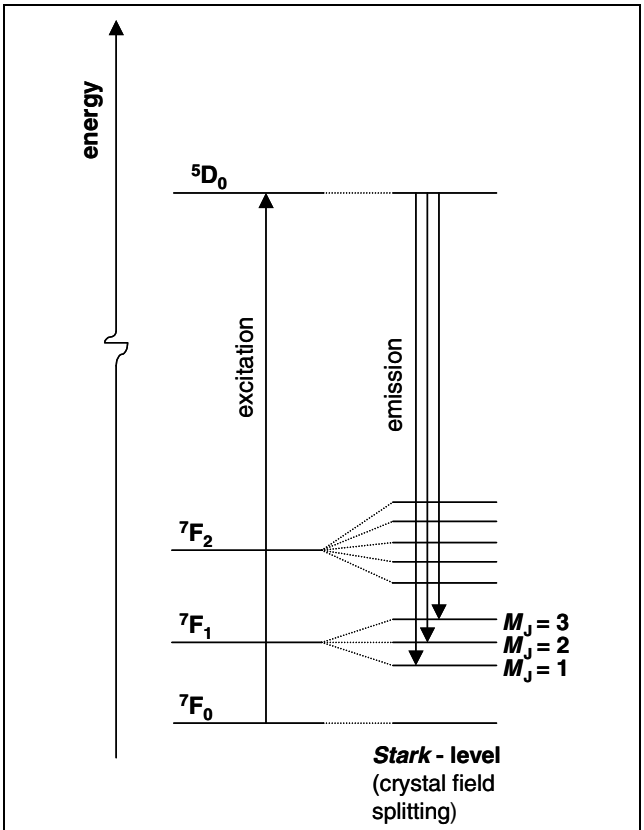

Figure 7. Part of the energy scheme of the Eu^{3+} ion, surrounded by a crystal field. The absorption and emission transitions correspond to those shown in Fig. 8.

Marmodée and co-workers [51] also observed a dependence of the energy of the Stark levels of the $^5D_0 \rightarrow {}^7F_1$ (see Fig. 8) and $^5D_0 \rightarrow {}^7F_2$ transitions (not shown) on the excitation wavelength. The slanted lines in the EEM show that there is a degree of correlation between the $^7F_0$ and $^7F_1$ levels, and that a long-wavelength excitation corresponds with a lower ligand field splitting. The splitting parameters were found to be highly characteristic for the particular complex.

Comparison of Eu(III) LLNS spectra in the presence of HS with spectra recorded in the presence of model compounds (hydroxy and methoxy benzoic acids) showed that, in HS, the dominant binding is via its carboxylate groups. Rather unexpectedly, no indication of chelate formation of the 2-hydroxy-benzoic acid type – in which the hydroxyl group also plays an important role – was detected [51].

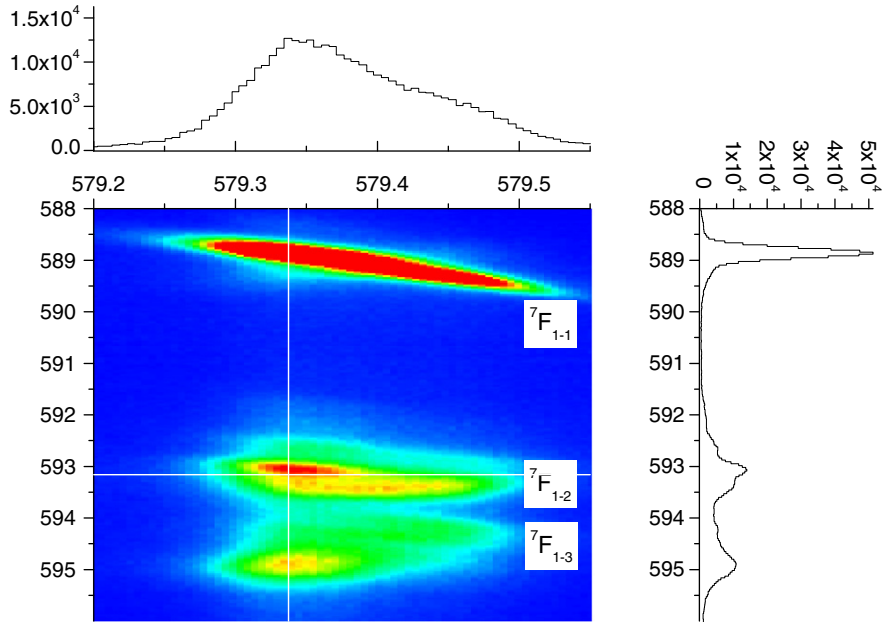

Figure 8. Excitation-emission matrix of the $^7F_1$ – multiplet of the Eu^3+ : 3MB = 1:1 mixture. Note the different scales of the excitation and emission dimensions; wavelengths in nm [51].

4. Summary

From the above, it can be concluded that FLNS has shown analytical potential, although the field of applicability still has to be further explored. In addition to the examples discussed above, it is expected that there will be many other fluorophores that exhibit fluorescence line-narrowing under cryogenic conditions.

The most powerful analytical feature of FLNS is fingerprint identification at very low concentrations in complex samples. It is mainly based on determining the vibrational frequencies of the S_1 state, which are shown to be quite sensitive for minor differences in chemical structures. Since libraries of FLN spectra are not available yet and theoretical methods to calculate precisely excited-state vibrations are still beyond the horizon, theoretical structure elucidation of unknown compounds on the basis of FLNS is not yet a realistic option, and standard reference compounds will often be required.

In addition to identification, the probing power of FLNS is quite fascinating, as demonstrated in this review. The S_1 vibrational frequencies are usually not affected by matrix interactions, but the relative intensities of the 0-0 multiplet lines and the intensity of the fluorescence background (PSB) are strongly influenced by the immediate environment of the fluorophore. Further exploration is needed because there is still little known about solvent dependency in FLNS. At present, only a qualitative interpretation is possible; a quantitative model to describe solvent effects adequately is lacking.

FLNS is applicable to a variety of matrices, allowing one to study the compound of interest in its ''natural'' environment. A basic assumption is that the cooling process from a liquid to an amorphous frozen matrix does not induce any major conformational changes. In most cases, this appears to be true [21,43]. In a few cases, alternative room temperature methods (e.g., fluorescence quenching or 2D-NMR) were available and supported the interpretation of the FLNS experiments [28].

We have demonstrated that FLNS can be used to study binding mode and conformation of PAH-DNA adducts, a highly relevant topic since certain conformations were found to be more quickly repaired than others. In the field of immuno-analytical chemistry, FLNS provided insight into the binding mode to MAbs, thus enhancing our understanding of important aspects, such as selectivity and cross-reactivity.

Thanks to its unique features, FLNS is expected to become a useful tool in binding studies of fluorescent ligands. The functional groups in a receptor-binding pocket, such as HIS or PHE, can be mimicked with specific solvent combinations and the spectra reveal which binding mode is predominant. Furthermore, many proteins containing porphyrin groups have been studied with FLNS in order to characterize their level of structure, and the technique was also applied to photosynthetic systems. Finally, an interesting new field is the use of LLNS to elucidate the binding mode of lanthanide ions to humic substances.

We expect that, with the availability of user-friendly tunable laser systems and closed-cycle refrigerators that

can reach temperatures of 4–5 K or fiber-optic probes that can simply be suspended in a helium storage dewar, more research groups will soon add this technique to their analytical toolbox and start to explore its exciting possibilities.

References

[1] B. Valeur, Molecular Fluorescence: Principles and Applications, Wiley, New York, USA, 2001.
[2] C. Gooijer, F. Ariese, J.W. Hofstraat (Editors), Shpol'skii spectroscopy and other site-selection methods, Wiley, New York, USA, 2000.
[3] R. Jankowiak, G.J. Small, Anal. Chem. 61 (1989) A1023.
[4] R. Jankowiak, G.J. Small, Chem. Res. Toxicol. 4 (1991) 256.
[5] R. Jankowiak, in: C. Gooijer, F. Ariese, J.W. Hofstraat (Editors), Shpol'skii spectroscopy and other site-selection methods, Wiley, New York, USA, 2000, pp. 235–271.
[6] P. Devanesan, F. Ariese, R. Jankowiak, G.J. Small, E.G. Rogan, E.L. Cavalieri, Chem. Res. Toxicol. 12 (1999) 796.
[7] R. Jankowiak, E.L. Cavalieri, E.G. Rogan, J. Phys. Chem. B 108 (2004) 10266.
[8] S. Yu, D.G. Gomez, A.D. Campiglia, Applied Spectrosc. 60 (2006) 1174.
[9] C. Gooijer, S.J. Kok, in: C. Gooijer, F. Ariese, J.W. Hofstraat (Editors), Shpol'skii spectroscopy and other site-selection methods, Wiley, New York, USA, 2000, pp. 307–331.
[10] K.P. Roberts, R. Jankowiak, G.J. Small, Anal. Chem. 73 (2001) 951.
[11] R. Jankowiak, K.P. Roberts, G.J. Small, Electrophoresis 21 (2000) 1251.
[12] K.M. Murdoch, J.C. Wright, in: C. Gooijer, F. Ariese, J.W. Hofstraat (Editors), Shpol'skii spectroscopy and other site-selection methods, Wiley, New York, USA, 2000, pp. 503–541.
[13] B. Henderson, Contemp. Phys. 43 (2002) 273.
[14] M. Mikami, T. Ueta, D. Kobayashi, A. Koreeda, S. Saikan, J. Lumin. 86 (2000) 257.
[15] C. Reichardt, Chem. Rev. 94 (1994) 2319.
[16] M. Orrit, J. Bernard, R.I. Personov, J. Phys. Chem. 97 (1993) 10256.
[17] I. Renge, U.P. Wild, in: C. Gooijer, F. Ariese, J.W. Hofstraat (Editors), Shpol'skii spectroscopy and other site-selection methods, Wiley, New York, USA, 2000, pp. 19–71.
[18] M. Lamotte, in: C. Gooijer, F. Ariese, J.W. Hofstraat (Editors), Shpol'skii spectroscopy and other site-selection methods, Wiley, New York, USA, 2000, pp. 73–114.
[19] C. Gooijer, I. Kozin, N.H. Velthorst, Mikrochim. Acta 127 (1997) 149.
[20] A.N. Bader, V.G. Pivovarenko, A.P. Demchenko, F. Ariese, C. Gooijer, J. Phys. Chem. B 108 (2004) 10589.
[21] J.M. Vanderkooi, in: C. Gooijer, F. Ariese, J.W. Hofstraat (Editors), Shpol'skii spectroscopy and other site-selection methods, Wiley, New York, USA, 2000, pp. 363–379.
[22] R.I. Personov, E.I. Al'Shits, L.A. Bykovskaya, B.M. Kharlamov, J. Exper. Theor. Phys. USSR 38 (1974) 912.
[23] R.I. Personov, in: C. Gooijer, F. Ariese, J.W. Hofstraat (Editors), Shpol'skii spectroscopy and other site-selection methods, Wiley Interscience, New York, USA, 2000, pp. 1–18.
[24] N.M. Grubor, R. Shinar, R. Jankowiak, M.D. Porter, G.J. Small, Biosens. Bioelectron. 19 (2004) 547.
[25] A.N. Bader, M.M. Van Dongen, M.M.H. Van Lipzig, J. Kool, J.H. Meerman, F. Ariese, C. Gooijer, Chem. Res. Toxicol. 18 (2005) 1405.
[26] A.J. Bystol, A.D. Campiglia, Appl. Spectrosc. 57 (2003) 697.
[27] M. Suh, R. Jankowiak, F. Ariese, B. Mao, N.E. Geacintov, G.J. Small, Carcinogenesis 15 (1994) 2891.
[28] M. Suh, F. Ariese, G.J. Small, R. Jankowiak, T.M. Liu, N.E. Geacintov, Biophys. Chem. 56 (1995) 281.
[29] M. Suh, F. Ariese, G.J. Small, R. Jankowiak, A. Hewer, D.H. Philips, Carcinogenesis 16 (1995) 2561.
[30] M. Banasiewicz, G. Nelson, A. Swank, N. Grubor, J. Ross, S. Nesnow, H. Köfeler, G.J. Small, R. Jankowiak, Anal. Biochem. 334 (2004) 390.
[31] S.D. Duhachek, J.R. Kenseth, G.P. Casale, G.J. Small, M.D. Porter, R. Jankowiak, Anal. Chem. 72 (2000) 3709.
[32] E.L. Cavalieri, E.G. Rogan, Pharmacol. Ther. 55 (1992) 183.
[33] S.J. Kok, R. Posthumus, I. Bakker, C. Gooijer, U.A.Th. Brinkman, N.H. Velthorst, Anal. Chim. Acta 303 (1995) 3.
[34] A.N. Bader, N.M. Grubor, F. Ariese, C. Gooijer, R. Jankowiak, G.J. Small, Anal Chem. 76 (2004) 761.
[35] J.M. Hayes, T. Reinot, N. Dang, G.J. Small, J. Phys. Chem. A 107 (2003) 10514.
[36] N.M. Grubor, Y. Liu, X. Han, D.W. Armstrong, R. Jankowiak, J. Am. Chem. Soc. 128 (2006) 6409.
[37] N.M. Grubor, J. Hayes, G.J. Small, R. Jankowiak, Proc. Natl. Acad. Sci. USA 102 (2005) 7453.
[38] G.D. Charles, M.J. Bartels, T.R. Zacharewski, B.B. Gollapudi, N.L. Freshour, E.W. Carney, Toxicol. Sci. 55 (2000) 320.
[39] M.M.H. Van Lipzig, N.P.E. Vermeulen, R. Gusinu, J. Legler, H. Frank, A. Seidel, J.H.N. Meerman, Environ. Toxicol. Pharmacol. 19 (2005) 41.
[40] A.C.W. Pike, A.M. Brzozowski, R.E. Hubbard, T. Bonn, A.-G. Thorsell, O. Engström, J. Ljunggren, J.A. Gustafsson, M. Carlquist, EMBO J. 18 (1999) 4608.
[41] G.M. Anstead, K.E. Carlson, J.A. Katzenellenbogen, Steroids 62 (1997) 268.
[42] M.M.H. Van Lipzig, A.M. Ter Laak, A. Jongejan, N.P.E. Vermeulen, M. Wamelink, D. Geerke, J.H.N. Meerman, J. Med. Chem. 47 (2004) 1018.
[43] J. Fidy, M. Laberge, A.D. Kaposi, J.M. Vanderkooi, Biochim. Biophys. Acta 1386 (1998) 331.
[44] A.D. Kaposi, W.W. Wright, J.M. Vanderkooi, J. Fluor. 13 (2003) 59.
[45] V. Logovinsky, A.D. Kaposi, J.M. Vanderkooi, Biochim. Biophys. Acta 1161 (1993) 149.
[46] K. Szőcs, G. Csík, A.D. Kaposi, J. Fidy, Biochim. Biophys. Acta 1541 (2001) 170.
[47] M. Laberge, M. Osvath, J. Fidy, Biochemistry 40 (2001) 9226.
[48] A. Gall, B. Robert, R.J. Cogdell, M.-C. Bellissent-Funel, N.J. Fraser, FEBS Lett. 491 (2001) 143.
[49] E.J.G. Peterman, H. Van Amerongen, R. Van Grondelle, J.P. Dekker, Proc. Natl. Acad. Sci. USA. 95 (1998) 6128.
[50] M.U. Kumke, F.H. Frimmel, F. Ariese, C. Gooijer, Environ. Sci. Technol. 34 (2000) 3818.
[51] B. Marmodee, J. De Klerk, M.U. Kumke, F. Ariese, C. Gooijer, J. Alloy. Compd. 451 (2008) 361 (unpublished results).
[52] F.H. Frimmel, G. Abbt-Braun, K.G. Heumann, B. Hock, H.-D. Lüdemann, in: M. Spiteller (Editor), Refractory Organic Substances (ROS) in the Environment, Wiley, New York, USA, 2002.
[53] F.S. Richardson, Chem. Rev. 82 (1982) 541.
[54] J.-C.G. Bünzli, in: J.-C.G. Bünzli, G.R. Choppin (Editors), Lanthanide Probes in Life, Chemical and Earth Sciences, Elsevier, Amsterdam, The Netherlands, 1989 Ch. 7.

Freek Ariese obtained his Ph.D. in 1993 at the Vrije Universiteit (VU) Amsterdam, The Netherlands, for his research on low-temperature fluorescence (Shpol'skii) spectroscopy, and the analysis of PAH metabolites in biological fluids. He then worked for three years as a postdoctoral fellow at Iowa State University, USA, using FLNS to identify adducts of carcinogenic PAHs with DNA and thus help elucidate the mechanisms of cancer initiation. After his return to

Amsterdam, he worked for three years at the Institute for Environmental Studies/IVM, focusing on the determination of environmental pollutants. He is currently associate professor at the Department of Analytical Chemistry and Applied Spectroscopy and at the Laser Centre VU. His main research interests are luminescence (including cryogenic approaches), Raman spectroscopy, cavity ring-down, and the coupling of advanced spectroscopic detection to chemical separations.

Arjen N. Bader obtained his Ph.D. in 2005 at the Vrije Universiteit Amsterdam for his research on fluorescent probes and their local environment studied under high-resolution, low-temperature conditions. Besides applying FLNS for probing protein-binding sites, his thesis also described environmental effects on proton-transfer reactions in 3-hydroxyflavone and its derivatives in Shpol'skii matrices. Currently, he is working as a postdoctoral fellow at Universiteit Utrecht, The Netherlands, focusing on the development and application of Förster resonance energy transfer (FRET) imaging techniques, in particular, homo-FRET imaging.

Cees Gooijer is Head of the Applied Spectroscopy group at the Laser Centre VU. He is an enthusiastic lecturer and is involved in (bio)-analytical and physical chemistry research. In analytical chemistry, his research focuses on spectroscopic detection and identification methods for LC and CE (in particular Raman spectroscopy and phosphorescence) and on cryogenic high-resolution luminescence. The focus in physical chemistry research is on complex biosystems (e.g., protein folding) by means of time-resolved fluorescence and Raman spectroscopy.